Urban climate and heat stress patterns in Berlin,Germany

Steffen Lauf[1], Pierre Adrienne Dugord[1], Birgit Kleinschmit[1]
[1] *Technische Universität Berlin,* Straße des 17. Juni 145
10623 Berlin, Germany*, steffen.lauf@tu-berlin.de*

15 June 2015

1. Introduction

Heat poses many challenges for human health as recently documented in many studies from different research fields (Epstein & Mills, 2005; Gabriel & Endlicher, 2011; Kovats & Hajat, 2008). While heat stress can be evaluated using concepts of hazard, vulnerability and risk; these terms are either vague or are focused on a distinct disciplinary perspective (Aubrecht & Özceylan, 2013; Kjellstrom, et al., 2007; Renn, 1998). According to IPCC (2012) and UNDRO (1980), risk defines the possibility of an adverse effect that can be described by a function of a physical hazard (i.e. heat) and the vulnerability of the exposed element (i.e. urbanities). On that basis, Scherer, et al. (2013) developed a feasible and transferable concept to quantify human heat stress risk in a study on Berlin. The statistical study revealed that for Berlin the total mortality risk was on average 5% higher during heat waves between 2001-2010 with a pronounced effect on those aged 64 years and older who were 6 times more vulnerable.

Besides the individual vulnerability affecting heat stress risk due the respective physical sensitivities and capabilities to adapt (Schuster, Honold, Lauf, & Lakes, 2015), the risk to be affected by heat stress involves a strong spatiotemporal dependency. On the one hand, the risk varies within the duration of the day and its accompanied activities, e.g. work, work/home travel, leisure, sleep; and on the other hand the risk differs across the urban landscape due to varying temperature patterns. Current studies found heat stress at night-time while sleeping is particularly dangerous when occurring over longer periods due to the often limited adaptation possibilities (Gabriel & Endlicher, 2011; Kovats & Hajat, 2008). In consequence, the crucial nocturnal regeneration phase is disturbed with potential stress effects reaching into the next day. The spatial variation of heat stress is strongly influenced by the spatial urban configuration, such as land use and land cover (LULC) and its respective capacity of cooling and shading or its intensity of thermal storage (Arnfield, 2003; Mathey, Rößler, Lehmann, & Bräuer, 2011). The urban environment has implications on the hazard side which is determined by the regional weather conditions (namely heat events) and its local extremes (e.g. urban heat islands).

In this study, we intended, firstly, to reveal functional relations between the urban configuration and varying temperature patters that crucially drive of urban heat stress, and secondly, to apply a heat stress risk model in which risk is determined by the components hazard and vulnerability spatially explicitly. At that, we distinguished between day and night-time heat stress due to significant differences in terms of adaptation towards heat stress reduction, which for instance at night is bonded to a fixed place, usually the bed room (Gabriel & Endlicher, 2011).

2. Method

Urban configuration and temperature patters

Utilising spectral imagery from remote sensing (Landsat 7 ETM) that includes thermal bands allowed us to gain citywide data at day and at night on the distribution of land surface temperature (LST) as one well-proven heat stress indicator (Small, 2006; Xu, Wooster, & Grimmond, 2008). Exemplarily two consecutive Landsat scenes were applied, 13th of August 2000 (10pm) and 14th of August 2000 (10am). We determined the structurally-driven variance for day and night-time temperatures. To make conclusion on how temperature patterns are influenced by the urban configuration, representative indicators had to be selected. We used LULC classes in combination with landscape metrics, and several urban classifiers, such as NDVI, surface sealing and building density for the city of Berlin. Using these parameters we could determine the relations between urban structure and urban heat and their differences between day and night (Dugord, Lauf, Schuster, & Kleinschmit, 2014). Statistical relations between temperature and urban patterns were carried out by applying Pearson correlations and linear regression on the level of urban neighbourhoods (cf. Fig. 3) using spatially-corrected mean values.

The heat stress risk model

The introduced concept that defines heat stress risk to be a function of vulnerability and hazard was applied spatially explicit on the Berlin building block level to reveal city-wide differences within micro-scale accuracy. By defining the vulnerability by the percentage of people equal to or greater than 65 years in age multiplied by the population density for each building block and by defining the hazard by the local mean night-time temperature deviation related to the same building blocks, we could derive the a priori heat stress risk at night for the city of

Berlin (Dugord, et al., 2014). In order to combine information on vulnerability and hazard and in order to transfer the risk concept, a simple normalization was chosen ranging from 0 to 10. Both factors were equally weighted to determine the final risk that again provided a maximum range of 10. The focus was on night-time heat stress due to its importance in terms of lower adaptation possibilities (cf. sect. 1; Schuster, et al., 2015).

3. Results

3.1 Urban configuration and temperature patters

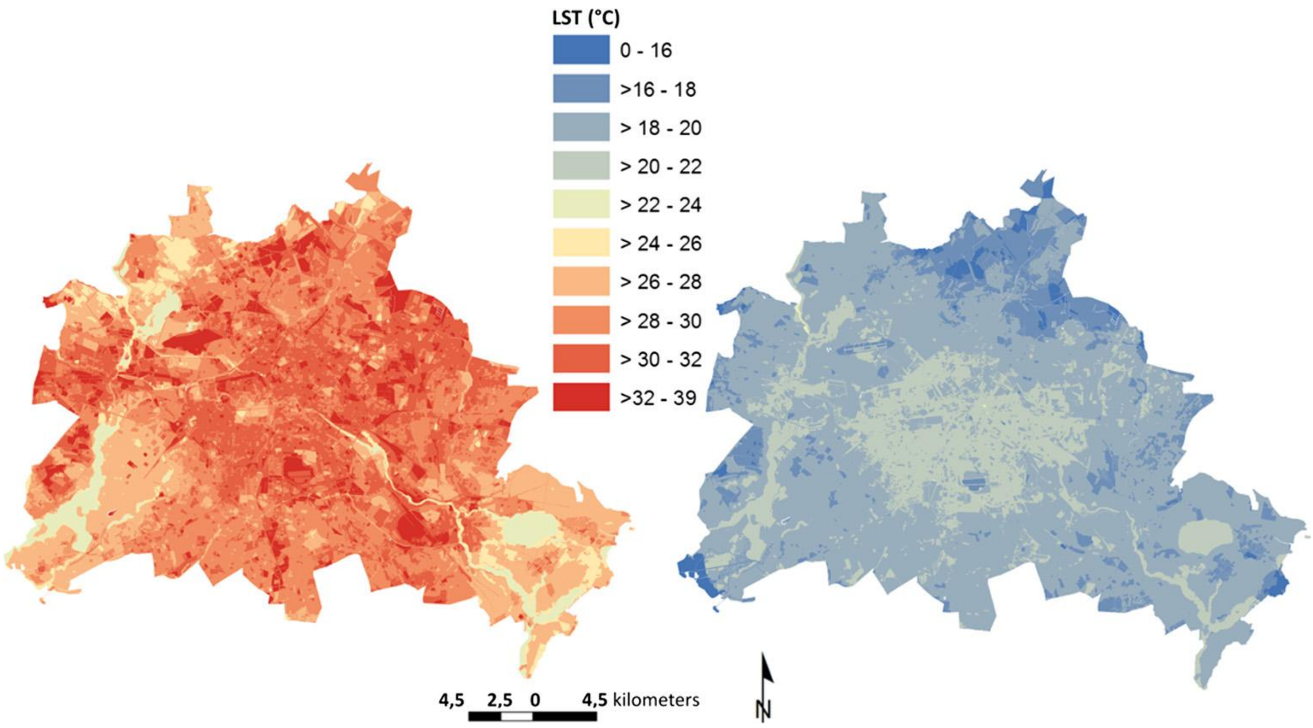

Significance levels of the p-values: '**' = 0.01; '*' = 0.05

Fig. 1 Berlin LST pattern in August at day (10am) and night (10pm).

The comparison of temperature patterns at day and night revealed significant differences. In the morning patches with the highest temperatures of over 30°C were randomly distributed across the administrative area of Berlin. The underlying LULC of these patches were agricultural land, open spaces and meadows. In these LULCs temperatures increased quickly with the beginning insolation due to shadeless exposition and low albedo values. The inertia of water resulted in the lowest temperatures in water bodies at 10am. A slight trend of temperature increase towards the center was, however, noticeable. The moderate increase was mainly due to building and vegetation shading. At 10pm a distinct urban heat island was noticeable. The reason was the general continual heat emission of built-up surfaces after insolation has stopped. This fact underlined the importance of considering heat stress at night when excess heat is only slowly discharged. During the day water bodies stored a large amount of thermal energy resulting in relatively high temperatures at night.

Tab. 1 Pearson's correlation coefficients between urban indicators and mean LSTs at 10am and 10pm.

	Structural indicators				*LULC-based indicators*				
	Degree of Sealing	*Floor Area Ratio*	*NDVI*	*Distance City Center*	*Transport Density*	*Extent Continuous*	*Extent Detached*	*Extent Green Space*	*Extent Water*
Mean LST 10am	.52**	.33**	-.53**	-.33**	.18**	.43**	-.28**	-.37**	-.40**
Mean LST 10pm	.71**	.60**	-.63**	-.54**	.41**	.59**	-.40**	-.35**	-.05

The statistical analysis testing the influence of the urban configuration (applying selected indicators) on LST revealed that at 10am high temperatures were statistically mainly related to high sealing rates, low NDVI values and a large extent of continuous urban fabric. At 10pm high temperatures were even stronger related to high sealing rates, low NDVI values and a large extent of continuous urban fabric, but additionally also to high floor area ratios which depicts the building density.

Tab. 2 Multiple and single linear regressions for mean LST and combined urban indicators at 10am and 10pm.

	Multiple R^2	***Degree of Sealing***	***Floor Area Ratio***	***NDVI***	***Distance City Center***	***Trans port Density***	***Extent Continu ous***	***Extent Detached***	***Extent Green Space***	***Extent Water***
***Mean** LST 10am*	.51***	.27***	.11***	.28***	.09*	.03**	/	.09***	.14***	.16***
Mean LST 10pm	.56***	.50***	.38*	.40**	.31 **	.17*	.35***	.16***	.12**	.002***

Table 2 represents all single linear regression results that were carried out for all urban indicator at 10am and 10pm. Moreover, multiple regression results are presented for ach point in time including all available and relevant indicators. The separate multiple regression analyses considering only structural indicators (degree of sealing, floor are ratio, NDVI and distance to the center) or LULC indicators (extent of continuous urban fabric, detached houses, green spaces and water, plus transportation density) revealed almost equal results at 10am ($R^2 \approx 0.37$). The combination of both increased the coefficient of determination of almost 15%. The exclusion of 'Extent Continuous' despite its stronger correlation coefficient strongly improved the model stability (model significance level and Akaike's information criterion). One reason was the strong correlations of it with almost all other indicators (except for extent of water and green space). At 10pm, the linear regression model with 'Degree of Sealing' as explanatory variable already explained 50% of LST variation; whereas all indicators together increased the coefficient of determination at only six percent. It could be proved that structural indicators and especially 'Degree of Sealing' explained LST's variation in Berlin better that LULC indicators at 10pm. These rather moderate results speak in favor for additional indicators driving LSTs. Kolokotroni and Giridharan (2008) for example found that the surface albedo was the most critical driver of outdoor temperatures in London (UK).

3.2 The heat stress risk model

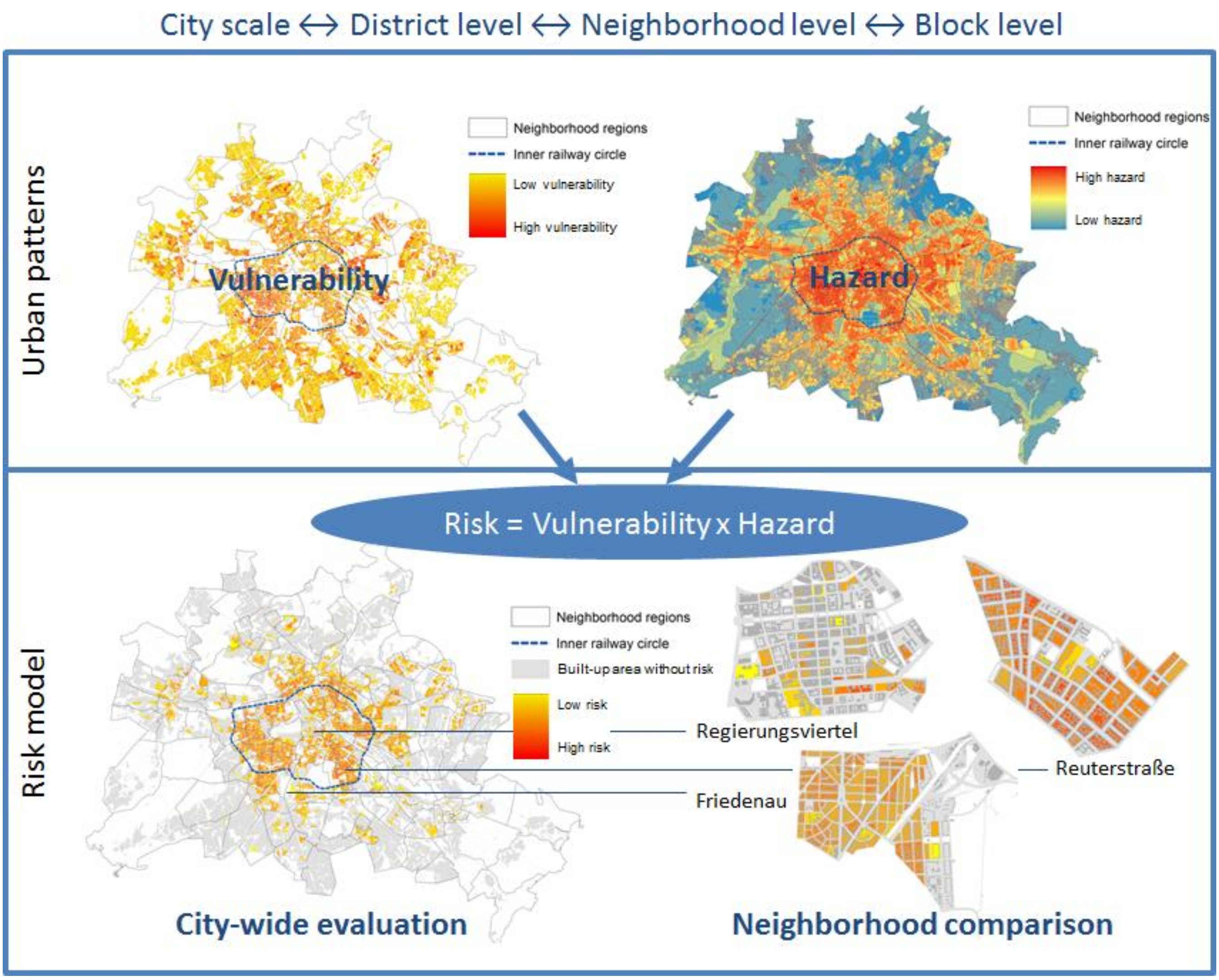

Fig. 2 Heat stress risk model output, above: the vulnerability and hazard pattern, below: the final patterns of heat stress risk with enlargements of selected neighborhoods

The results showed unexpected risk patterns with higher risks in less central and less dense neighborhoods, and lower risks in very dense neighborhoods. These insights affirmed the risk concept and the idea of combining relevant information on the vulnerability and the hazard side to identify areas at risk in terms of heat stress.

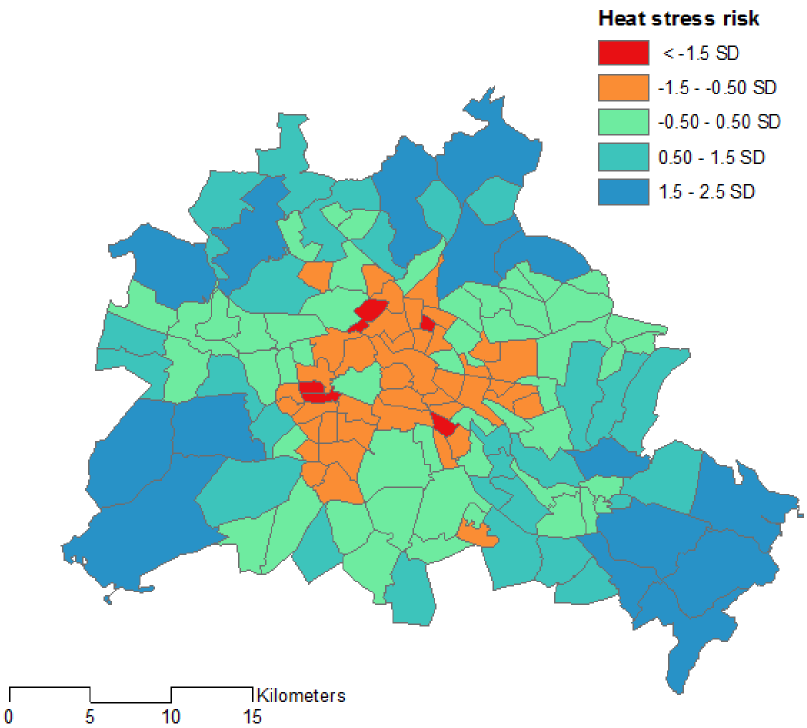

Fig. 3 Heat stress risk at the neighborhood level

Besides the risk representation on the building block level, results could also be provided on the neighborhood level (Figure 3). This enables a comparison of different spatial scales and allows for a stepwise analysis of heat stress risk along different planning levels. The identified risk pattern provides consistency with underlying LULC. Neighborhoods with a negative deviation from the regional mean match inner-city structures with a high building density, mainly consisting of five to six story perimeter constructions from Wilhelminian times. These structures also provide a relatively high population density. Areas with highly positive deviations on the city edge consist of large forested green space. For the large amount of detached and semi-detached building constructions (family homes) also a positive standard deviation was ascertained. An overview of the statistical distribution of normalized heat stress risk vales is given in Figure 4.

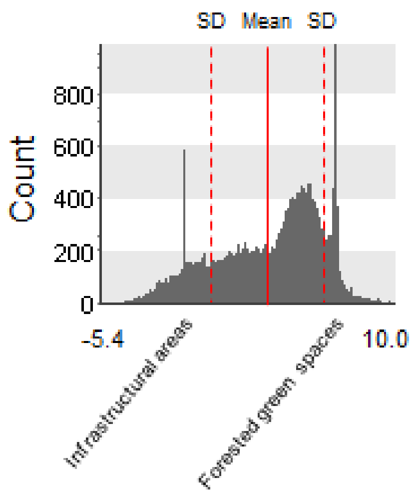

	Block (n=25414)	Neighborhood (n=138)
Mean	3.4	2.2
SD	2.8	2.1
Max	10.0	6.7
Min	-5.4	-1.8

Fig. 4 Comparing the statistical heat stress risk distribution among the block and neighborhood level

4. Discussion and Conclusion

To gain a more thorough understanding of the interrelation between urban configurations and local climate, and how it might vary over time, e.g. under severe heat events, multi-temporal approaches seem promising to explore significant differences in event-based temperature patterns. In the ongoing project ‘Urban Climate and Heat

Stress in mid-latitude cities' we currently consider mean summer temperature distributions distinguished between inside and outside of occurred heat events and distinguished between day and night-time within a multi-temporal approach. This analysis will help to determine the crucial effects of heat events on the interface of urban structure and local climate.

The presented heat stress risk model revealed interesting insights to assist resilient urban planning regarding heat stress adaptation. In this context actions of adaptation can, firstly, address vulnerability, for instance, by reducing the number of vulnerable people with a high physical sensitivity from locations of high risks (e.g. by promoting institutional relocation of retirement homes) or by reducing the exposure of people, for example, by installing air conditioning systems. Secondly, the local hazard can be addressed by changing the local environmental settings, e.g. by increasing vegetation density with street trees, roof or facade greenery (Gill, et al., 2008), or by directing urban development while taking into account the insights of the aforementioned structural and LULC-related influences on LST variance. The creation of new urban green spaces can acts on both sides; on the hazard side by cooling through evapotranspiration and reducing sensitive thermal radiation and on the vulnerability side by reducing population density due to lowering potential urban concentration. This risk model might additionally serve as an instrument to test the effectiveness of single actions of adaptation to reduce heat stress risks because changes of hazard or vulnerability related indicators can be tested systematically. For the determination of the efficiency of single actions, possible side effects need to be linked and considered holistically. For that purpose the integration of actions into the concept of (multiple) ecosystem services seems promising (Lauf, Haase, & Kleinschmit, 2014).

However, for a dynamic consideration of heat stress risks as well as risk adaptation, combined model approaches are needed, especially with regard to future developments. In Western societies' urban populations are projected to increase while population ageing continues, putting more people at risk of heat stress in cities (Scherer, et al., 2013). Heat waves, which are projected to increase in frequency and intensity in the 21st century, further aggravate the already elevated air temperatures in cities as the result of climate change (IPCC, 2012). The combination of urban structural and population dynamics with climate and risk modelling enables a long-term consideration of heat stress risks under climatic and urban changes, which becomes relevant in terms of forward-looking adaptation.

Acknowledgment

We want to thank the German Research Foundation for funding the project "Urban Climate and Heat Stress in Mid-latitude Cities, UCaHS" and Dieter Scherer for putting this group together.

References

Arnfield, A. J. (2003). Two decades of urban climate research: A review of turbulence, exchange of energy, water and the urban heat islands. *International Journal of Climatology, 2* (1), 1-26.

Aubrecht, C., & Özceylan, D. (2013). Identification of heat risk patterns in the U.S. National Capital Region by integrating heat stress and related vulnerability. *Environment International, 56* (0), 65-77.

Dugord, P.-A., Lauf, S., Schuster, C., & Kleinschmit, B. (2014). Land use patterns, temperature distribution, and potential heat stress risk – The case study Berlin, Germany. *Computers, Environment and Urban Systems, 48* (0), 86-98.

Epstein, P. R., & Mills, E. (2005). Climate change futures: health, ecological and economic dimensions. In. Center for Health and the Global Environment, Harvard Medical School, Boston, MA.

Gabriel, K. M. A., & Endlicher, W. R. (2011). Urban and rural mortality rates during heat waves in Berlin and Brandenburg, Germany. *Environmental Pollution, 159* (8–9), 2044-2050.

Gill, S. E., Handley, J. F., Ennos, A. R., Pauleit, S., Theuray, N., & Lindley, S. J. (2008). Characterising the urban environment of UK cities and towns: A template for landscape planning. *Landscape and Urban Planning, 87* (3), 210-222.

IPCC. (2012). *Managing the Risks of Extreme Events and Disasters to Advance Climate Change Adaptation*. Cambridge University Press, Cambridge, UK, and New York, NY, USA.

Kjellstrom, T., Friel, S., Dixon, J., Corvalan, C., Rehfuess, E., Campbell-Lendrum, D., Gore, F., & Bartram, J. (2007). Urban environmental health hazards and health equity. *Journal of urban health, 84* (1), 86-97.

Kolokotroni, M., & Giridharan, R. (2008). Urban heat island intensity in London: An investigation of the impact of physical characteristics on changes in outdoor air temperature during summer. *Solar Energy, 82* (11), 986-998.

Kovats, R. S., & Hajat, S. (2008). Heat Stress and Public Health: A Critical Review. *Annual Review of Public Health, 29*, 41-55.

Lauf, S., Haase, D., & Kleinschmit, B. (2014). Linkages between ecosystem services provisioning, urban growth and shrinkage – A modeling approach assessing ecosystem service trade-offs. *Ecological Indicators, 42* (0), 73-94.

Mathey, J., Rößler, S., Lehmann, I., & Bräuer, A. (2011). Urban green spaces - Potentials and constraints for urban adaptation to climate change In K. Otto-Zimmermann (Ed.), *Resilient cities. Cities and Adaptation to Climate Change. Proceedings of the Global Forum 2010. Dordrecht [u.a.]* (pp. 479-485). Springer, Berlin.

Renn, O. (1998). Three decades of risk research: accomplishments and new challenges. *Journal of Risk Research, 1* (1), 49-71.

Scherer, D., Fehrenbach, U., Lakes, T., Lauf, S., Meier, F., & Schuster, C. (2013). Quantification of heat stress hazards, vulnerabilities and risks in cities – The example of heat-stress related mortality in Berlin, Germany. *die Erde, 144* (3-4), 238-259.

Schuster, C., Honold, J., Lauf, S., & Lakes, T. (2015). Urban heat stress linked to health and fitness: implications for alternative adaptation strategies. *Global Environmental Change, submitted*.

Small, C. (2006). Comparative analysis of urban reflectance and surface temperature. *Remote Sensing of Environment, 104*, 168-189.

UNDRO. (1980). Natural disasters and vulnerability analysis. In *Report of Expert Group Meeting (9-12 July 1979).* Geneva.

Xu, W., Wooster, M. J., & Grimmond, C. S. B. (2008). Modelling of urban sensible heat fux at multiple spatial scales: A demonstration using airborne hyperspectral imagery of Shanghai and a temperature–emissivity separation approach. *Remote Sensing of Environment, 112*, 3493-3510.